

Comparative Evaluation of Single- and Multi-Marker Pose Estimation for Freehand 3D Ultrasound Reconstruction

Syahid Al Irfan and Oky Dicky Ardiansyah Prima

Graduate School of Software and Information Science, Iwate Prefectural University

152-52 Sugo, Takizawa, Iwate, Japan

Email: s236x002@s.iwate-pu.ac.jp, prima@iwate-pu.ac.jp

Abstract—This study evaluates marker-based pose estimation methods for freehand three-dimensional (3D) ultrasound reconstruction by comparing single-marker and multi-marker configurations and analyzing their effects on reconstruction accuracy and pose stability. Although vision-based fiducial markers provide a low-cost and compact alternative to optical or electromagnetic tracking systems, their performance can degrade due to occlusion, motion blur, and variations in viewing angle. To improve robustness, multi-marker rigs arranged on polyhedral structures maintain visibility across multiple faces. In this study, both configurations were calibrated to a shared coordinate system and applied to breast-phantom data containing spherical inclusions with known diameters (5 mm and 10 mm). Ultrasound images and marker-tracking videos were recorded simultaneously, and each frame was paired with its corresponding six-Degree-of-Freedom (6-DoF) pose for volumetric reconstruction. The reconstructed inclusions were segmented and compared with ground-truth volumes, and statistical analysis was conducted using two-way Analysis of Variance (ANOVA) with object diameter and tracking methods as factors. The results show that multi-marker tracking consistently reduced volumetric error and variability, achieving the lowest mean error of 12.1 mm³ for 5-mm inclusions, whereas the single-marker configuration produced larger errors, particularly for 10-mm inclusions. ANOVA revealed significant main effects for both diameter and tracking methods. These findings indicate that multi-marker configurations improve pose robustness and enhance reconstruction accuracy in freehand 3D ultrasound systems.

Keywords-Freehand 3D ultrasound; Pose estimation; Multi-marker tracking; Volumetric reconstruction.

I. INTRODUCTION

3D ultrasound reconstruction generates volumetric datasets by spatially assembling sequential two-dimensional brightness mode (B-mode) images according to the position and orientation of the ultrasound probe [1]. In freehand 3D ultrasound systems, accurate pose estimation is essential to ensure that each acquired frame is correctly positioned within a global coordinate system. The overall reconstruction accuracy, therefore, depends not only on image quality but also critically on the precision and stability of the probe-tracking method.

Various tracking technologies have been employed in freehand 3D ultrasound, including optical infrared systems, electromagnetic sensors, and vision-based tracking approaches [2]. Although optical and electromagnetic systems can provide high accuracy, they often involve high cost, complex installation, and susceptibility to environmental

interference. Vision-based fiducial marker tracking using printed markers, such as ArUco offers a compact and low-cost alternative [3]. However, single-marker tracking is vulnerable to occlusion, motion blur, and variations in viewing angle or illumination [4], which may result in unstable corner detection and cumulative pose drift during reconstruction [5]. Such instability can directly degrade volumetric reconstruction accuracy.

To mitigate these limitations, multi-marker fiducial configurations have been proposed. By arranging multiple markers on different faces of a three-dimensional object, multi-marker rigs increase the probability that at least one marker remains visible under challenging viewing conditions [6]. Systems such as DodecaPen have demonstrated that multi-marker configurations can achieve highly accurate six-Degree-of-Freedom (6-DoF) tracking using a monocular camera [7]. Despite these advantages, the effectiveness of multi-marker tracking for improving volumetric reconstruction accuracy in freehand 3D ultrasound has not been systematically evaluated, particularly for small, cancer-like targets.

Mammography remains the standard imaging modality for breast cancer screening. However, its diagnostic sensitivity is significantly reduced in women with dense breast tissue, where overlapping fibroglandular structures can obscure lesions [8]. To address this limitation, Automated Breast Ultrasound (ABUS) has been introduced as a standardized, operator-independent three-dimensional (3D) ultrasound technique [9]. Clinical studies have demonstrated that supplementing mammography with ABUS improves cancer detection in women with dense breasts, reporting an additional detection rate of 2.4 cancers per 1,000 screened women [10] and an increase in diagnostic performance, with the Area Under the Curve (AUC) improving from 0.72 to 0.82, and sensitivity increasing by 29% [11]. These findings highlight the clinical importance of volumetric ultrasound imaging.

Consequently, this study seeks to compare single-marker and multi-marker pose estimation approaches in the context of freehand 3D ultrasound reconstruction. We hypothesize that multi-marker configurations provide significantly improved reconstruction accuracy and stability compared to single-marker tracking. To test this hypothesis, experiments were conducted using breast phantoms containing spherical inclusions of known diameters (5 mm and 10 mm). Reconstruction accuracy was evaluated by volumetric error analysis and statistically examined using two-way Analysis of Variance (ANOVA).

By quantitatively analyzing the influence of marker configuration and object size, this study provides

experimental evidence regarding the effectiveness of multi-marker tracking for low-cost freehand 3D ultrasound systems.

Relevant literature on the topic of implementing marker detection for 3D reconstruction, along with the necessary information to investigate for a deeper understanding of the topic are summarized in Section II. The details on the data collection methods and how the two types of markers for 3D ultrasound reconstruction are evaluated, along with their implementation, are explained in Section III. Finally, the results obtained from the experiment, the conclusions that can be drawn, and the discussions are summarized in Sections IV to VI.

II. RELATED WORKS

Several studies on the use of markers as anchors for pose estimation have shown that the use of multi-marker systems provides advantages, especially in terms of reducing detection ambiguity and improving the stability of jittery marker detection [12]. In another study related to the use of multi-marker [13], it is shown that marker configurations arranged in a 3D non-coplanar structure, such as in a dodecahedron-shaped object, provide improved accuracy and stability of pose estimation compared to planar configurations. This is due to the ability of the 3D configuration to provide geometric constraints from multiple orientations, thereby reducing the ambiguity that commonly occurs in coplanar arrangements, even when multiple markers are used with uniform orientation relative to the camera.

Studies that utilize markers as pose-estimation tools and apply them for 3D ultrasound reconstruction have been conducted, demonstrating strong potential. One work directly related to the fundamental development of marker-based pose estimation is the research by Wu et al. [7] in which they developed a system called DodecaPen. The system uses multiple ArUco markers arranged on a dodecahedron structure and projects the global reference points to the stylus-tip position. Their results showed that they achieved high measurement accuracy, with the lowest translation-vector error reaching 0.34 mm. However, the study did not provide a comparative evaluation between multi-marker and single-marker approaches for tip projection.

Another relevant work related to 3D ultrasound reconstruction was conducted by Léger et al. [14]. In their study, they used only a single ArUco marker attached to the ultrasound probe. To enhance marker-detection accuracy, they used a RealSense RGB camera as the marker-capturing sensor. For evaluation, they designed a phantom experiment using LEGO blocks and wires placed between them. The phantom was then submerged in water as the ultrasound medium. The reconstructed wire length was compared to the ground-truth wire length, producing errors of 2.64 mm, 1.50 mm, and 13.83 mm along the x , y , and z axes, respectively. However, the study did not evaluate reconstruction performance on small objects representing cancer-like lesions.

Marker-based pose estimation for 3D ultrasound was also implemented by De Sanctis et al. [3]. They designed a 3D ultrasound system utilizing a dodecahedron-shaped marker as the pose reference. To obtain a reference measurement for comparison, an infrared tracking system was employed. The marker and infrared tracker were positioned on opposite sides of the ultrasound beam to ensure visibility. To assess performance, they conducted reconstruction tests on phantoms constructed using 3D-printed bone structures and tissue-mimicking material. The system achieved average errors of 0.857, 0.453, and 2.689 mm along the x , y , and z axes, respectively. However, like previous works, they did not investigate reconstruction performance on small cancer-representative objects.

III. METHOD

In the process of 3D reconstruction using marker-based ultrasound, the stability of pose measurement through marker detection becomes crucial in determining the accuracy of the reconstruction results. Although a single marker is easy to implement, it has limitations at extreme angles. Study shows that multi-marker approaches are more robust under extreme angles [13], but they introduce additional complexity in terms of design and implementation. In this study, an experimental workflow will be conducted to evaluate the accuracy of reconstruction results by collecting quantitative data from both single-marker and multi-marker approaches. The overall workflow of the proposed experimental framework is illustrated in Figure 1.

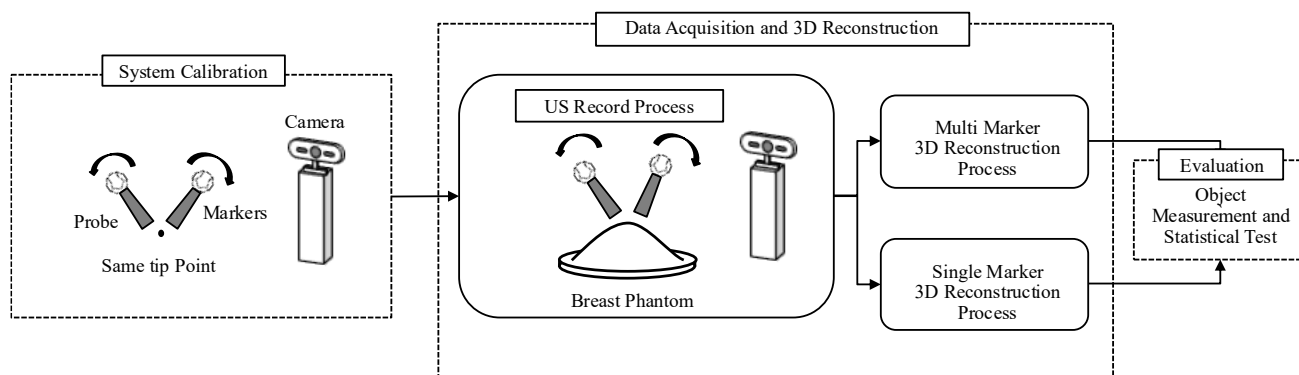


Figure 1. Overview of the proposed experimental workflow.

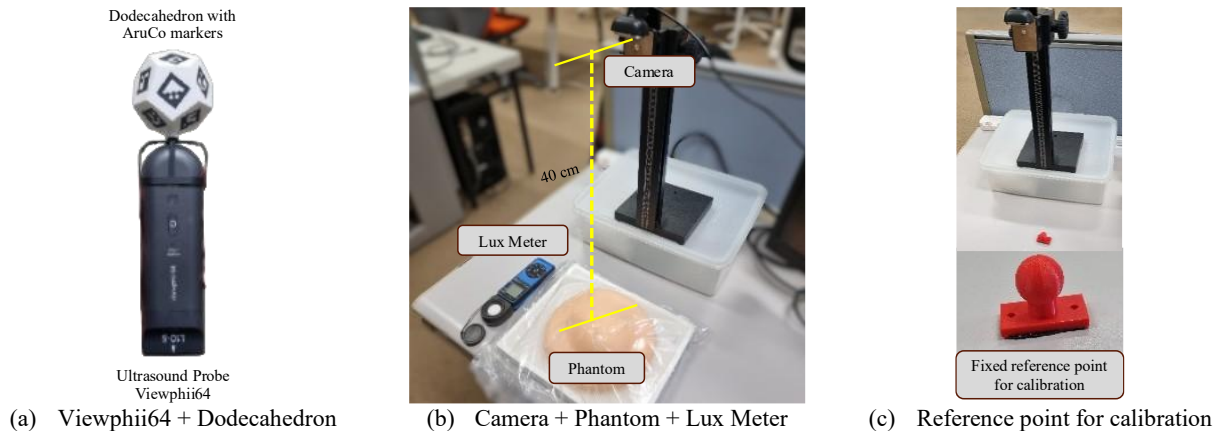


Figure 2. Experimental setup for freehand 3D ultrasound reconstruction.

A. Experimental Setup

The experimental system consisted of an ultrasound probe equipped with either a single ArUco marker or a dodecahedron-shaped multi-marker structure. In the single-marker configuration, one marker from the same marker set used in the multi-marker structure was selected to maintain geometric consistency between conditions. The ultrasound imaging device used in this study was the Viewphii64 system (Socionext, Japan) [15], which provides real-time B-mode imaging suitable for freehand acquisition. A monocular RGB camera [16] was mounted approximately 40 cm above the acquisition area to capture marker motion during scanning. Illumination was maintained at approximately 500 Lux to minimize detection variability caused by lighting changes.

A commercial breast phantom [17] containing spherical inclusions with known diameters of 5 mm and 10 mm was used as the reconstruction target. Ultrasound B-mode images were acquired while the camera simultaneously recorded marker motion for pose estimation. This synchronized acquisition enabled pairing each ultrasound frame with its corresponding 6-DoF pose.

The detailed hardware configuration is shown in Figure 2. As illustrated in Figure 2(a), the fiducial marker structure was rigidly attached to the probe on the side opposite to the ultrasound emission surface to avoid acoustic interference while ensuring continuous visibility from the overhead camera. Figure 2(b) presents the overall data acquisition environment, where the RGB camera was positioned vertically above the phantom to provide a stable field of view and minimize perspective distortion during tracking.

In addition, Figure 2(c) shows the fixed reference point used during the calibration procedure. This reference point was placed within the acquisition area and served as a spatial anchor for probe-tip projection validation. During calibration, the probe tip was repeatedly aligned with this fixed reference while the marker was moved in various orientations. Consistent projection of the probe-tip position to the same global coordinate confirmed proper alignment between the tracking system and the ultrasound image plane. The inclusion of this fixed reference ensured that calibration accuracy was evaluated under reproducible geometric conditions.

B. Calibration Procedure

To ensure a fair comparison between configurations, each tracking method was calibrated independently while being aligned to a common global coordinate system. The calibration process included camera intrinsic calibration, marker size calibration, and probe-tip offset calibration. The probe-tip position was defined relative to the marker coordinate system to establish a consistent spatial relationship between pose estimation and the ultrasound image plane.

Calibration accuracy was verified by projecting the probe tip to a fixed reference point in the acquisition area. Consistent projection results across repeated probe movements indicated successful calibration. This procedure ensured that any differences observed in reconstruction accuracy were attributable to the tracking configuration rather than misalignment or calibration bias.

C. Data Acquisition

Following calibration, data acquisition was conducted under controlled scanning conditions. For each configuration, ultrasound B-mode images and corresponding marker-tracking video were recorded simultaneously. Each ultrasound frame was associated with its estimated 6-DoF pose derived from marker detection.

To reduce variability in reconstruction results, probe motion was performed slowly and consistently in a single direction. By minimizing the spatial gap between consecutive frames, this approach ensures denser sampling, which is crucial for improving interpolation accuracy and overall 3D reconstruction quality [18].

D. 3D Reconstruction and Volume Measurement

Three-dimensional reconstruction was performed by placing each B-mode image frame in 3D space according to its estimated pose. All processing was conducted using 3D Slicer [19] with Python scripting to ensure reproducibility. The spherical inclusions within the phantom were segmented semi-automatically, and volumetric measurements were computed from the segmented regions.

Segmentation results were visually inspected to identify potential errors. When necessary, manual corrections were

applied to ensure measurement reliability. This hybrid segmentation approach was adopted to balance automation and accuracy.

Reconstruction accuracy was evaluated by comparing the measured volume of each inclusion with its known ground-truth volume. The volumetric error for object i was defined as

$$e_i = |V_{measured,i} - V_{actual,i}|$$

where $V_{measured,i}$ denotes the reconstructed volume and $V_{actual,i}$ represents the true volume. Smaller error values indicate higher reconstruction accuracy.

E. Statistical Analysis

To determine whether marker configuration and object size significantly affected reconstruction accuracy, a two-way ANOVA was performed. The independent variables were marker configuration (single-marker versus multi-marker) and object diameter (5 mm versus 10 mm), while the dependent variable was volumetric reconstruction error. Each configuration is tested with 10 repetitions, where smaller error values indicate better performance. The data collection was performed using one type of breast phantom, carried out by a single operator who does not have a medical background.

Statistical significance was defined at a threshold of $p < 0.05$. If significant main effects or interactions were observed, further analysis was conducted to interpret differences between experimental conditions. Through this structured analysis, the study systematically evaluates the influence of tracking configuration and object size on volumetric reconstruction performance.

IV. RESULTS

A. Calibration Accuracy

Prior to reconstruction experiments, calibration accuracy was evaluated to ensure that both tracking configurations were properly aligned within the same global coordinate system. The average probe-tip projection error under approximately 500 Lux illuminations was (0.64, 0.02, 0.63) mm for the multi-marker configuration and (0.22, 0.23, 0.91) mm for the single-marker configuration.

B. Volumetric Reconstruction Accuracy

After calibration, 3D reconstruction experiments were conducted for spherical inclusions with diameters of 5 mm and 10 mm. Volumetric errors were calculated by comparing reconstructed volumes with ground-truth values. Table I shows our volumetric reconstruction errors for single-marker and multi-marker configurations.

For the 5-mm inclusions, the multi-marker configuration achieved a mean volumetric error of 12.1 mm³, whereas the single-marker configuration produced substantially larger errors with greater variability. The standard deviation was notably lower in the multi-marker condition, indicating improved stability.

For the 10-mm inclusions, reconstruction errors increased in both configurations. However, the difference between tracking methods became more pronounced. The single-marker configuration exhibited the largest mean error (132.7

mm³) and higher variability, while the multi-marker configuration maintained comparatively lower error values.

Overall, the results demonstrate that multi-marker tracking consistently reduced volumetric error and improved measurement stability across object sizes.

C. Statistical Analysis

To determine whether the observed differences were statistically significant, a two-way ANOVA was performed with marker configuration and object diameter as independent factors (Table II).

The analysis revealed a highly significant main effect of object diameter ($F = 86.02, p < 0.001$), indicating that reconstruction accuracy differed substantially between 5-mm and 10-mm inclusions. A significant main effect of marker configuration was also observed ($F = 6.34, p = 0.016$), demonstrating that tracking method significantly influenced volumetric reconstruction accuracy.

TABLE I. VOLUMETRIC RECONSTRUCTION ERRORS FOR SINGLE-MARKER AND MULTI-MARKER CONFIGURATIONS

| Diameter (mm) | Volume (mm ³) | Error (Measured - Actual) | | | | | |
|---------------|---------------------------|---------------------------------|------|--------|----------------------------------|-------|--------|
| | | Multi Marker (mm ³) | | | Single Marker (mm ³) | | |
| | | <i>e</i> | Avg | StdDev | <i>e</i> | Avg | StdDev |
| 5 | 65.5 | 8.9 | 12.1 | 9.7 | 23 | 18.5 | 9.1 |
| | | 24.9 | | | | | |
| | | 15.1 | | | | | |
| | | 31.3 | | | | | |
| | | 3.2 | | | | | |
| | | 7.9 | | | | | |
| | | 10.1 | | | | | |
| | | 14.7 | | | | | |
| | | 0.3 | | | | | |
| | | 4.7 | | | | | |
| 10 | 523.6 | 143.2 | 87.6 | 29.1 | 227.6 | 132.7 | 56.2 |
| | | 92.8 | | | | | |
| | | 59.3 | | | | | |
| | | 73.3 | | | | | |
| | | 71.4 | | | | | |
| | | 69.9 | | | | | |
| | | 65.2 | | | | | |
| | | 134.9 | | | | | |
| | | 92.2 | | | | | |
| | | 74.2 | | | | | |

TABLE II. COMPARISON OF VOLUMETRIC RECONSTRUCTION ERRORS BETWEEN TRACKING CONFIGURATIONS

| Source | DF | F | p-value |
|-------------------|----|-------|------------|
| Diameter | 1 | 86.02 | <0.001 *** |
| Method | 1 | 6.34 | 0.016 * |
| Diameter × Method | 1 | 3.57 | 0.067 |
| Error | 36 | — | — |

*, $p < 0.05$, **, $p < 0.01$ (), ***, $p < 0.001$

The interaction between object diameter and marker configuration approached significance ($F = 3.57, p = 0.067$) but did not reach the 0.05 threshold. This suggests that while reconstruction error increases with object size, the relative advantage of multi-marker tracking remains consistent across diameters.

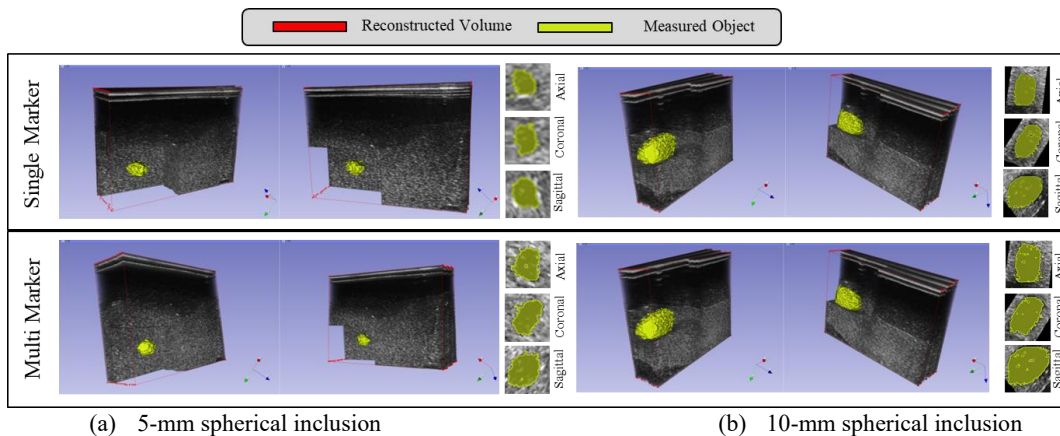


Figure 3. Representative 3D reconstruction results.

These statistical findings quantitatively confirm that multi-marker tracking provides measurable improvements in reconstruction accuracy.

D. Qualitative Reconstruction Comparison

Representative reconstruction results are presented in Figure 3 for both 5-mm and 10-mm spherical inclusions. For the 5-mm inclusions, both tracking configurations were able to reconstruct the general spherical structure; however, the multi-marker configuration exhibited smoother surface boundaries and more consistent spatial alignment. In contrast, the single-marker reconstruction showed minor boundary irregularities and slight positional inconsistencies, reflecting small pose fluctuations during scanning.

For the 10-mm inclusions, the qualitative differences between configurations became more apparent. The multi-marker reconstruction maintained a relatively uniform surface shape and coherent volumetric structure. Conversely, the single-marker reconstruction displayed noticeable surface distortions and irregular volume expansion, suggesting the accumulation of pose estimation errors over the scanning trajectory. These distortions are consistent with the larger quantitative errors observed in the volumetric measurements.

V. DISCUSSION

A. Interpretation of Reconstruction Accuracy

The experimental results demonstrate that the multi-marker configuration significantly improved volumetric reconstruction accuracy compared to the single-marker configuration. This improvement can be primarily attributed to enhanced pose stability during freehand scanning. In single-marker tracking, pose estimation relies on the visibility and geometric consistency of a single planar marker. When the marker experiences unfavorable viewing angles, corner detection accuracy degrades, leading to instability in pose estimation and accumulated reconstruction error.

In contrast, the multi-marker configuration provides redundant geometric constraints. Because markers are distributed across multiple faces of a polyhedral structure, at least one marker remains visible under most viewing

conditions. This redundancy stabilizes pose estimation and reduces jitters in 6-DoF tracking, an effect that is supported by the observed reduction in variability in volumetric measurements.

B. Influence of Object Size

The results also show that reconstruction error increased significantly for 10-mm inclusions, indicating greater sensitivity of larger objects to cumulative pose drift during scanning. Despite this size dependence, the multi-marker configuration consistently reduced errors, with no significant interaction effect, demonstrating robust performance across object diameters and spatial scales.

C. Engineering Implications

From an engineering perspective, pose stability is critical in freehand 3D ultrasound, as small angular errors can accumulate into significant spatial inaccuracies. Multi-marker configurations provide a low-cost, robust solution to improve tracking stability using simple hardware, making them suitable for portable and resource-limited clinical settings.

D. Clinical Relevance

Although this study was conducted using a breast phantom, the findings have implications for clinical ultrasound imaging. In breast cancer screening, accurate volumetric reconstruction may improve lesion visualization and measurement reproducibility. While automated systems such as ABUS provide standardized volumetric imaging, freehand 3D ultrasound remains attractive due to its flexibility and lower hardware complexity. Improving tracking robustness through multi-marker configurations could help bridge the gap between low-cost freehand systems and more sophisticated automated platforms.

E. Limitations

Several limitations should be considered when interpreting the results. First, the experiments were conducted under controlled lighting conditions with approximately 500 Lux illuminations. Marker detection performance may vary under different clinical lighting environments. Second, only two object sizes were evaluated, limiting the analysis of scale-

dependent reconstruction behavior. Third, segmentation included manual correction, which may introduce minor observer-dependent variability. The fourth limitation lies in the type of phantom used and the limited number of data points per testing type, which is only 10, resulting in low data variability and limiting the precision of the findings across several scenarios.

Another limitation comes from a Human-Computer Interaction (HCI) perspective, where the design places a 50 g 3D-printed model on top of the ultrasound probe shifts the center of gravity of that device. This creates a unique challenge in ensuring that the added weight does not impose extra burden or discomfort on the operator during use. Another HCI-related challenge involves maintaining the marker-equipped dodecahedron within an optimal distance of 10–15 cm from the camera to ensure stable pose estimation.

VI. CONCLUSION AND FUTURE WORK

This study quantitatively compares single-marker and multi-marker pose estimation methods for freehand three-dimensional (3D) ultrasound reconstruction using a controlled breast-phantom experiment. The results demonstrated that multi-marker tracking significantly improves volumetric reconstruction accuracy and stability compared to single-marker tracking, with the smallest error observed for the 5-mm inclusions reaching 12.1 mm³. Similar findings related to using multiple sensor configurations can be found in other studies [20], which shows that using multiple sensors of the same type has better accuracy and stability for 3D ultrasound reconstruction.

Two-way ANOVA confirmed significant main effects of both object diameter and tracking configuration on reconstruction error, providing statistical evidence that marker arrangement directly influences volumetric accuracy. Although reconstruction errors increased for larger objects, the relative advantage of multi-marker tracking remained consistent across object sizes.

These findings highlight the importance of pose robustness in freehand 3D ultrasound systems. Even when calibration precision is comparable, dynamic tracking stability plays a critical role in reconstruction accuracy. Multi-marker configurations provide a practical and low-cost solution to enhance pose estimation without requiring expensive tracking hardware.

REFERENCES

- [1] P.-W. Hsu, R. W. Prager, A. H. Gee, and G. M. Treece, "Freehand 3D Ultrasound Calibration: A Review," in *Advanced Imaging in Biology and Medicine*, C. W. Sensen and B. Hallgrímsson, Eds., Berlin, Heidelberg: Springer Berlin Heidelberg, 2009, pp. 47–84. doi: 10.1007/978-3-540-68993-5_3.
- [2] W. He *et al.*, "Freehand 3D Ultrasound Imaging Based on Probe-mounted Vision and IMU System," *Ultrasound in Medicine & Biology*, vol. 50, no. 8, pp. 1143–1154, 2024, doi: <https://doi.org/10.1016/j.ultrasmedbio.2024.03.021>.
- [3] L. De Sanctis, A. Carnevale, C. Antonacci, E. Faiella, E. Schena, and U. G. Longo, "Six-Degree-of-Freedom Freehand 3D Ultrasound: A Low-Cost Computer Vision-Based Approach for Orthopedic Applications," *Diagnostics*, vol. 14, no. 14, p. 1501, Jul. 2024, doi: 10.3390/diagnostics14141501.
- [4] W. He *et al.*, "Freehand 3D Ultrasound Imaging Based on Probe-mounted Vision and IMU System," *Ultrasound in Medicine and Biology*, vol. 50, no. 8, pp. 1143–1154, Aug. 2024, doi: 10.1016/j.ultrasmedbio.2024.03.021.
- [5] C. A. Adriaans, M. Wijkhuizen, L. M. Van Karnenbeek, F. Geldof, and B. Dashtbozorg, "Trackerless 3D Freehand Ultrasound Reconstruction: A Review," *Applied Sciences*, vol. 14, no. 17, p. 7991, Sep. 2024, doi: 10.3390/app14177991.
- [6] P. García-Ruiz, F. J. Romero-Ramírez, R. Muñoz-Salinas, M. J. Marín-Jiménez, and R. Medina-Carnicer, "Fiducial Objects: Custom Design and Evaluation," *Sensors*, vol. 23, no. 24, p. 9649, Dec. 2023, doi: 10.3390/s23249649.
- [7] P.-C. Wu *et al.*, "DodecaPen: Accurate 6DoF Tracking of a Passive Stylus," in *Proceedings of the 30th Annual ACM Symposium on User Interface Software and Technology*, Québec City QC Canada: ACM, Oct. 2017, pp. 365–374. doi: 10.1145/3126594.3126664.
- [8] W. A. Berg, E. A. Rafferty, S. M. Friedewald, C. B. Hruska, and H. Rahbar, "Screening Algorithms in Dense Breasts: *AJR* Expert Panel Narrative Review," *American Journal of Roentgenology*, vol. 216, no. 2, pp. 275–294, Feb. 2021, doi: 10.2214/AJR.20.24436.
- [9] I. Boca (Bene), A. I. Ciurea, C. A. Ciordea, and S. M. Ducea, "Pros and Cons for Automated Breast Ultrasound (ABUS): A Narrative Review," *JPM*, vol. 11, no. 8, p. 703, Jul. 2021, doi: 10.3390/jpm11080703.
- [10] B. Wilczek, H. E. Wilczek, L. Rasouliyan, and K. Leifland, "Adding 3D automated breast ultrasound to mammography screening in women with heterogeneously and extremely dense breasts: Report from a hospital-based, high-volume, single-center breast cancer screening program," *European Journal of Radiology*, vol. 85, no. 9, pp. 1554–1563, Sep. 2016, doi: 10.1016/j.ejrad.2016.06.004.
- [11] M. L. Giger *et al.*, "Automated Breast Ultrasound in Breast Cancer Screening of Women With Dense Breasts: Reader Study of Mammography-Negative and Mammography-Positive Cancers," *American Journal of Roentgenology*, vol. 206, no. 6, pp. 1341–1350, Jun. 2016, doi: 10.2214/AJR.15.15367.
- [12] G. Čepon, D. Očepek, M. Kodrič, M. Demšar, T. Bregar, and M. Boltežar, "Impact-Pose Estimation Using ArUco Markers in Structural Dynamics," *Exp Tech*, vol. 48, no. 2, pp. 369–380, Apr. 2024, doi: 10.1007/s40799-023-00646-0.
- [13] P. Oščádal *et al.*, "Improved Pose Estimation of Aruco Tags Using a Novel 3D Placement Strategy," *Sensors*, vol. 20, no. 17, p. 4825, Aug. 2020, doi: 10.3390/s20174825.
- [14] É. Léger, H. E. Gueziri, D. L. Collins, T. Popa, and M. Kersten-Oertel, "Evaluation of Low-Cost Hardware Alternatives for 3D Freehand Ultrasound Reconstruction in Image-Guided Neurosurgery," in *Simplifying Medical Ultrasound*, vol. 12967, J. A. Noble, S. Aylward, A. Grimwood, Z. Min, S.-L. Lee, and Y. Hu, Eds., in Lecture Notes in Computer Science, vol. 12967, Cham: Springer International Publishing, 2021, pp. 106–115. doi: 10.1007/978-3-030-87583-1_11.
- [15] "ViewPhii64." [Online]. Available: <https://viewphii.com/viewphii64/about/index.html> 2026.04.14
- [16] "Microsoft LifeCam HD-3000." [Online]. Available: <https://www.microsoft.com/en-au/d/lifecam-hd-3000/8Q49LGBW0R58/?activetab=pivot:overviewtab> 2026.04.14
- [17] "Breast Phantom from OST Cooperation." Accessed: Apr. 14, 2026. [Online]. Available: <https://www.ost-jp.com/>
- [18] Q. Huang, M. Lu, Y. Zheng, and Z. Chi, "Speckle suppression and contrast enhancement in reconstruction of freehand 3D ultrasound images using an adaptive distance-weighted method," *Applied Acoustics*, vol. 70, no. 1, pp. 21–30, Jan. 2009, doi: 10.1016/j.apacoust.2008.02.002.
- [19] "3D Slicer." [Online]. Available: <https://www.slicer.org> 2026.04.14
- [20] M. Luo *et al.*, "Multi-IMU with Online Self-consistency for Freehand 3D Ultrasound Reconstruction," in *Medical Image Computing and Computer Assisted Intervention – MICCAI 2023*, vol. 14220, H. Greenspan, A. Madabhushi, P. Mousavi, S. Salcudean, J. Duncan, T. Syeda-Mahmood, and R. Taylor, Eds., in Lecture Notes in Computer Science, vol. 14220, Cham: Springer Nature Switzerland, 2023, pp. 342–351. doi: 10.1007/978-3-031-43907-0_33.